

# INFLUENCE OF INITIAL BED TEMPERATURE ON BED PERFORMANCE OF AN ADSORPTION REFRIGERATION SYSTEM

*Mr. Anirban SUR<sup>\*</sup>, Dr. Randip K. DAS<sup>1</sup>, Mr. Ramesh P. SAH<sup>2</sup>*

<sup>\*1</sup>Assistant Professor, Department of Mechanical Engg, Inderprasatha Engineering College, Ghaziabad, Uttar Pradesh, India.

<sup>2</sup>Professor, Department of Mechanical Engg, Indian School of Mines, Dhanbad, Jharkhand, India.

<sup>3</sup>Research Scholar, Department of Mechanical Engineering, Indian School of Mines, Dhanbad (India)

<sup>\*</sup>Corresponding author; E-mail: anirbansur26@gmail.com

**Abstract:** *The study deals with the complete dynamic analysis (numerical and practical) of an existing adsorption refrigeration system. The adsorption refrigeration setup is available at Indian School of Mines (Dhanbad, India) Mechanical engineering department. The system operates with activated carbon (as an adsorbent) and methanol (as refrigerant). Numerical model is established base on energy equation of the heat transfer fluid (water) and transient heat and mass transfer equations of the adsorbent bed. The input temperature of heat source is 90°C, which is very low compared to other low-grade energy input refrigeration system. The thermo-physical properties of an adsorptive cooling system (using activated carbon–methanol pair) are considered in this model. In this analysis influence of initial bed temperature ( $T_1$ ) on the bed performances are analysed mathematically and experimentally. The simulation and practical results of this system show that the cycle time decreases with increase in initial bed temperature and the minimum cycle time is 10.74 hours (884min for practical cycle) for initial bed temperature of 40°C. Maximum system COP and specific cooling capacity are 0.436 and 94.63kJ/kg of adsorbent under a condenser and evaporator temperatures of 35°C and 5°C, respectively. This analysis will help to make a comparison between simulated and experimental results of a granular bed adsorption refrigeration system and also to meet positive cooling needs in off-grid electricity regions.*

**Key words:** *Adsorption; Refrigeration; Activated-Carbon; Methanol; Dynamic simulation; Performance.*

## 1. Introduction:

Refrigerator driven by low-grade thermal energy from different sources is receiving much attention in recent years due to limited storage and environmental issues of fossil fuels. The traditional vapour compression refrigeration cycles strongly increase the consumption of electricity and generate serious environmental problem by the use of CFC/HFC/HCFC refrigerant. The adsorption refrigeration system is one of the promising refrigeration methods due to their uses of environment-friendly refrigerants along with less moving parts, silent operation and low maintenance requirements [1-3].

Many researchers conducted with adsorption refrigeration through either theoretical analysis or prototypes experimental works or the both [4]. Despite the above effort, detailed information on the modeling of heat and mass transfer in the adsorption refrigeration module is limited. In order to further investigate the characteristic of the module, a modified adsorption cooling model is designed in the current study and detailed study of heat and mass transfer performance is presented. It is hoped that such a study will lead to optimizing the design of the module, for the commercial availability and to encourage its wide spread application.

In this present study, an adsorption refrigeration system has been designed with activated carbon as adsorbent and methanol as the adsorbate. Activated carbon with methanol as a working pair is broadly used in adsorption refrigeration due to the large adsorption quantity (0.45 kg/ kg), low desorption heat (1800–2000 kJ /kg), chemical stability, very less corrosive, low cost and easy availability [4]. The properties of methanol indicate that it is a good choice as adsorbate in adsorption cooling because of its high latent heat (1102kJ/kg), easy adsorbability by adsorbent due to small molecular size, low specific volume, sub-atmospheric evaporation temperature, compatibility with copper [5-8].

## **2. System Description:**

The schematic diagram of the designed adsorption refrigeration system is shown in Fig. 1. It has five main components, namely, adsorber/desorber bed, condenser, receiver, expansion valve and evaporator. The adsorbent is packed in the adsorber/desorber bed in which the refrigerant gets adsorbed at a low temperature and pressure. It is desorbed at high temperature and pressure. There are a number of copper tubes running axially through the bed for alternately circulating hot and cold water. The adsorbent in the bed is heated by hot water (supplied from electric geyser) during desorption and cooled by circulating cold water through tubes during adsorption.

Initially, the bed is heated with the refrigerant remaining adsorbed in the bed and pressure inside the sealed container increasing gradually. When the desired level of pressure (equal to the condenser pressure) is reached, desorption starts and the desorbed refrigerant flows to the condenser. The rate of desorption is dependent on the bed temperature and the concentration of the adsorbed mass in the bed. During the desorption process, heat is required to be transferred to the bed to increase the bed temperature and also to provide heat for desorption. Therefore, hot water is circulated through the adsorber bed to supply the heat required by the bed. In the process, the bed reaches the point of maximum temperature. At this point, desorption is stopped and the adsorber bed is cooled with valves closed. The pressure inside the sealed container decreases till it reaches a value equal to the evaporator pressure. At this point, adsorption of refrigerant in the bed starts.

The vapour refrigerant desorbed from the bed is condensed to a liquid in the condenser and gets collected in the receiver. From the receiver, the liquid refrigerant is passed through the expansion valve and enters into the evaporator at the desired level of low temperature and pressure. The refrigerant evaporates in the evaporator while absorbing the latent heat from the water to be chilled. The vaporized refrigerant/adsorbate then enters the adsorber bed (which is already cooled and at the point of evaporator pressure) and gets adsorbed into a solid matrix of the adsorbent surface by secondary bonding. The process of cooling is continued during the adsorption process to reduce the bed temperature and also to absorb the heat of adsorption. Therefore, cold water is circulated through the adsorber bed to absorb the heat released from the bed. In the process, the bed regains its initial state [5]. Tab. 1 shows details of different components used for adsorption refrigeration system.

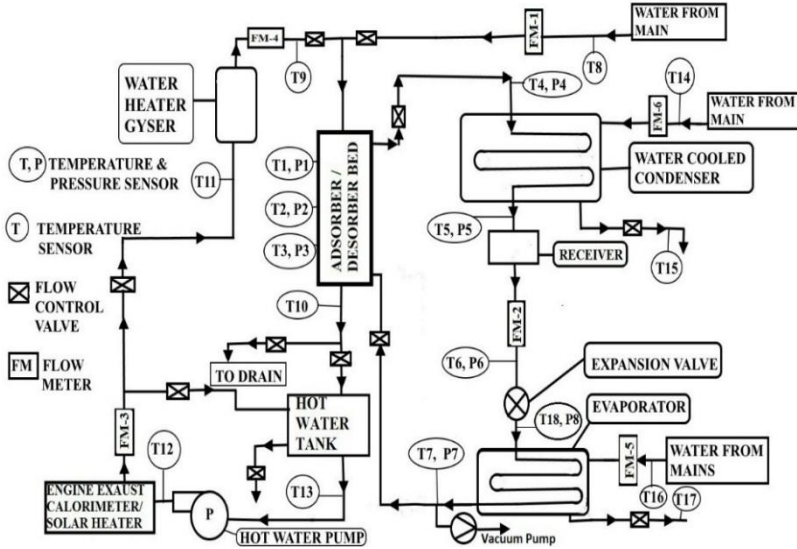


**Figure 1. Schematic Diagram [5] of the Adsorption Refrigeration System**

**Table 1. Details of component;**

Component	Dimension
Adsorber bed	Inner Dia 300 mm Length 1m
Condenser	Outer Dia 300 mm Length 1m
Evaporator	Length 500mm Outer Dia 125 mm
Receiver	Outer dia 100mm Length 260mm
Hot Water Tank	300Ltr capacity
Geyser	50Ltr capacity
Copper Tube pitch	17.5 (Square pitch)
Copper tube	Inner Dia 10 mm Outer Dia 12mm

### 3. Mathematical Model:

To find the influence of bed temperature on the simulated performance of the existing adsorption refrigeration, following energy balance equations are derived for different parts (adsorber/ desorber bed, condenser, evaporator) of adsorption system. A simulation code, written in FORTRAN, is employed in order to solve the algebraic heat and mass transfer equations. Fig.2 represents different thermodynamic processes of adsorption refrigeration.

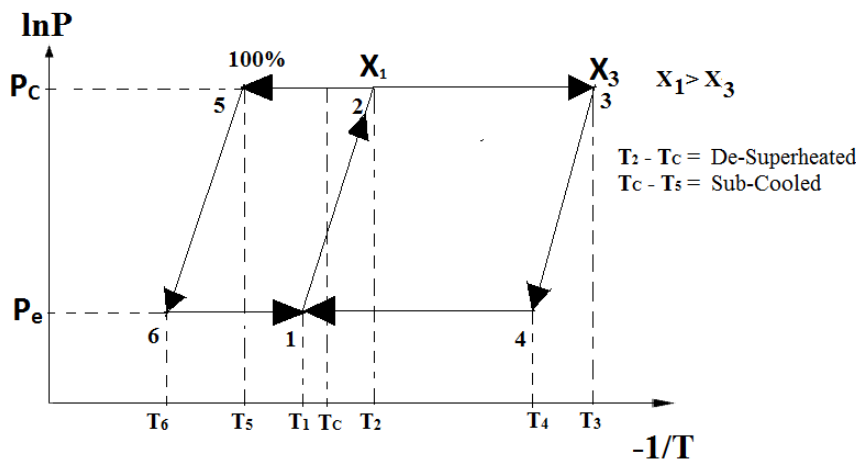


**Figure 2. P-T-X diagram for a basic adsorption system [5]**

The mathematical model that is built for this system are as follows:

#### 3.1 Heat transfer between heat transfer fluid and adsorber bed:

The rate of heat loss ( $\dot{Q}_h$ ) by the hot water flowing through the adsorber bed at any instant of time can be written as:

$$\dot{Q}_h = \dot{m}_{hw}c_{pw}(T_{hwi} - T_{hwo}) \quad (1)$$

$T_{hwo}$  can be estimated as follows by the help of LMTD heat exchanger equation:

$$T_{hwo} = T + (T_{hwi} - T)\exp^{-\left(\frac{U_oA_o}{\dot{m}_{hw}c_{pw}}\right)} \quad (2)$$

### 3.2 Governing equations for different processes in desorber/adsorber bed:

In this study, modified Dubinin-Astakhov(D-A) equation [6] is adopted to express the concentration  $x$  of the adsorbate as a function of temperature  $T$  and pressure  $P$ .

$$x(T, T_s) = x_o(T_s)\exp\left[-k\left(\frac{T}{T_{sat}}-1\right)^n\right] \quad (3)$$

The mass fraction,  $x$ , is defined as:  $X = \frac{\text{adsorbed mass of adsorbate}}{\text{mass of adsorbent}} \text{kg/kg}$  (4)

**3.2.1 Process 1-2 (Isosteric Heating):** The process is shown in Fig. 2 by the line 1-2. The desorber bed initially (at point 1 in Fig. 2) is at evaporator pressure  $P_E$  and temperature  $T_1$ , filled with adsorbed adsorbate. During this process, the adsorbed/desorber bed is heated with constant adsorbate mass ratio ( $x = x_1$ ), from an initial temperature of  $T_1$  to a temperature  $T_2$ , when the pressure of the bed reaches to the condensation pressure (i.e.,  $P_2 = P_C$ ). The rates of sensible heat gain during this process can be estimated as the sum of sensible heat gain by adsorbed refrigerant, by the adsorbent and by the bed materials. Therefore, the rate of heat transfer during this process can be written as:

$$(\dot{Q})_{1-2} = (m_{ab}c_{ab} + m_{ac}x_1c_{vref})\frac{dT}{dt} = \dot{m}_{hw}c_{pw}(T_{hwi} - T)\left(1 - \left(\exp^{-\left(\frac{U_oA_o}{\dot{m}_{hw}c_{pw}}\right)}\right)\right) \quad (5)$$

where,  $[m_{ab}c_{ab} = m_{st}c_{st} + m_{cu}c_{cu} + m_{ac}c_{ac}]$

Equating  $(\dot{Q})_{1-2}$  with the rate of heat loss by the circulating hot water ( $\dot{Q}_h$ ) [eq. (1). and eq. (2).]

$T_2$  can be calculated by equating the adsorbate mass ratios at points 1 and 2 ( $x_1$  and  $x_2$ ), and estimating them by using eq. (3).

$$T_2 = T_C \left[ 1 + \sqrt[n]{\left(\frac{T_1}{T_E} - 1\right)^n - \frac{1}{k} \ln \frac{x_o(T_E)}{x_o(T_C)}} \right] \quad (6)$$

**3.2.2 Isobaric desorption process (2-3):** The desorption process is represented by line 2-3 in Fig. 2. After achieving the condensation pressure ( $P_C$ ), desorption of refrigerant. During this process, the bed is heated from  $T_2$  to the maximum bed temperature of  $T_3$  while the pressure of the bed remains constant (at  $P_C$ ). Since desorption of refrigerant takes place, the adsorbed mass fraction,  $x$ , reduces as the process progresses and the instantaneous value of  $x$  is a function of time or temperature of the bed. Total heat transfer during this process is the sum of the sensible heat gain by the adsorbent, adsorber bed materials and refrigerant and the heat of desorption required for desorption of refrigerant.

Therefore, the energy equation during this process can be written as:

$$(\dot{Q})_{2-3} = (m_{ac}x(T) \cdot c_{p,ref} + m_{ab}c_{ab}) \frac{dT}{dt} + h_{id}m_{ac} \frac{dx}{dt} = \dot{m}_{hw}c_{pw}(T_{hwi} - T) \left( 1 - \exp^{-\left(\frac{U_oA_o}{\dot{m}_{hw}c_{pw}}\right)} \right) \quad (7)$$

Where,  $\Delta h_{id}$  is the heat of desorption per kg of desorbed refrigerant, which can be estimated as:

$$\Delta h_{id} = R \cdot C \frac{T}{T_s} \quad (8)$$

T is the instantaneous temperature of the bed during the process 2 – 3, and  $T_s$  is the saturation temperature corresponding to the bed pressure during desorption, which can be taken as equal to  $T_C$ , R is the gas constant for the refrigerant and C is the constant of Clausius –Clapeyron equation.

The rate of desorption of refrigerant,  $\left(\frac{dx}{dt}\right)$  is estimated from D-A equation as given in eq. (3). as

$$\frac{dx}{dt} = \frac{dx}{dT} \cdot \frac{dT}{dt} = \left[ \frac{(x(T,T_C) \cdot (-k) \times n)}{T_C} \left( \frac{T}{T_C} - 1 \right)^{n-1} \right] \frac{dT}{dt} \quad (9)$$

**3.2.3 Isosteric cooling Process (3-4):** Like the heating process, the concentration of adsorbate remains constant in isosteric cooling but at the minimum concentration value ( $x_{min}$ ) as shown by line 3–4 (Fig.2). During this process, the bed is cooled with constant adsorbed mass fraction from the maximum temperature  $T_3$  to a temperature  $T_4$ , when the pressure of the bed reaches to value equal to the saturation pressure ( $P_E$ ) of refrigerant corresponding to the evaporator temperature. The total heat lost during this process is summation of heat losses from the refrigerant, adsorbent and bed materials and can be estimated as:

$$(\dot{Q})_{3-4} = (m_{ac}x_3 \cdot c_{v,ref} + m_{ab}c_{ab}) \frac{dT}{dt} = \dot{m}_{cw}c_{pw} \left[ (T_{cwi} - T) \left( 1 - \exp^{-\left(\frac{U_oA_o}{\dot{m}_{cw}c_{pw}}\right)} \right) \right] \quad (10)$$

The temperature  $T_4$  can be calculated by equating the adsorbate mass ratios at points 3 and 4 ( $x_3$  and  $x_4$ ), as follows:

$$T_4 = T_E \left[ 1 + \sqrt[n]{\left(\frac{T_3}{T_C} - 1\right)^n - \frac{1}{k} \ln \frac{x_o(T_C)}{x_o(T_E)}} \right] \quad (11)$$

**3.2.4 Process 4-1 (Isobaric Cooling and Adsorption):** During this constant pressure cooling process, the temperature of bed reduces from  $T_4$  to  $T_1$  and the adsorbed mass fraction of refrigerant in the bed increases from  $x_4$  to  $x_1$  due to adsorption of refrigerant vapour coming out from the evaporator. Heat transfer during this process is the sum of (i) the sensible heat transfers from the adsorbent, adsorber bed materials and refrigerant, (ii) the heat of adsorption released during adsorption of refrigerant and (iii) the heat absorbed by the evaporated refrigerant which leaves the evaporator at temperature  $T_6$  and gets adsorbed in the bed at temperature T ( $T > T_6$ ).

Thus, the total heat loss during this process can be calculated as:

$$\begin{aligned}
(\dot{Q})_{4-1} &= (m_{ac}x \cdot c_{p,ref} + m_{ab}c_{ab}) \frac{dT}{dt} + h_{ia}m_{ac} \frac{dx}{dt} + (T - T_6)m_{ac}c_{p,ref} \frac{dx}{dt} \\
&= \dot{m}_{cw}c_{pw} \left[ (T_{cwi} - T) \left( 1 - \exp^{-\left(\frac{U_oA_o}{\dot{m}_{cw}c_{pw}}\right)} \right) \right]
\end{aligned} \tag{12}$$

where,  $\Delta h_{ia}$  is heat of adsorption per kg of adsorbed refrigerant, which can be estimated as:

$$\Delta h_{ia} = R \cdot C \frac{T}{T_s} \tag{13}$$

$T$  is the instantaneous temperature of the bed during the process 4 – 1, and  $T_s$  is the saturation temperature corresponding to the bed pressure during adsorption, which can be taken as equal to  $T_E$ .

The solution of the above equations gives (i) the instantaneous rates of temperature change and heat transfer to the bed, (ii) the instantaneous rate of mass transfer and total mass transfer during any process, and (iii) total heat transfer to the bed and the time required to complete the process.

**3.3 Heat transfer in condenser:** In the condenser, the desorbed refrigerant is first de-superheated from temperature  $T$  to the saturation temperature ( $T_C$ ) corresponding the condenser pressure and then condensed to saturated liquid and may be sub-cooled to a temperature lower than  $T_C$  ( Fig.2). Since, mass flow rate of refrigerant entering to the condenser is  $\left(m_{ac} \frac{dx(T,T_C)}{dt}\right)$ , the rate of heat rejection in the condenser can be estimated as follows:

$$(\dot{Q})_{COND} = m_{ac} \cdot \frac{dx(T,T_C)}{dt} [h_{ref}(T, P_C) - h_{ref}(T_C, P_C) + L_{ref}(T_C) + c_{p,liq}(T_C - T_5)] \tag{14}$$

where  $c_{p,liq}$  is specific heat of liquid refrigerant and  $T_5$  is the exit temperature of the refrigerant from the condenser. The total heat lost in the condenser during the whole cycle can be estimated as:

$$\begin{aligned}
(Q)_{COND} &= \int_{T_2}^{T_3} m_{ac} \frac{dx(T,T_C)}{dT} [h_{ref}(T, P_C) - h_{ref}(T_C, P_C)] dT + m_{ac}(x_1 - x_3)[L_{ref}(T_C) + \\
&c_{p,liq}(T_C - T_5)]
\end{aligned} \tag{15}$$

**3.4 Heat Transfer in Evaporator:** Refrigerant may be assumed to enter the evaporator with an enthalpy of  $h_5$ , at which it leaves the condenser. In the evaporator, the refrigerant absorbs heat from the space / substance to be cooled and evaporated to a saturated vapour. There is a possibility for the refrigerant vapour to be superheated up to temperature  $T_6$  before leaving the evaporator (Fig.2). Therefore, the rate of heat transfer in the evaporator (cooling power) is given by:

$$(\dot{Q})_{EVP} = m_{ac} \frac{dx(T, T_E)}{dt} [h_{ref}(T_E, P_E) - h_5 + c_{p,ref}(T_6 - T_E)] \tag{16}$$

where,  $h_{ref}(T_E, P_E)$  is the enthalpy of saturated vapour of refrigerant at pressure of  $P_E$  or temperature  $T_E$ .

Total refrigeration effect during one complete cycle can be estimated as:

$$(Q)_{EVP} = m_{ac}(x_1 - x_3)[h_{ref}(T_E, P_E) - h_5 + c_{p,ref}(T_6 - T_E)] \quad (17)$$

Specific Cooling Capacity (SCC) of the cycle is the ratio of total cooling effect in evaporator and the adsorbent mass and is estimated as:

$$SCC = \frac{Q_{EVP}}{m_{ac}} \quad (18)$$

Coefficient of Performance (COP) of the cycle is the ratio of total cooling effect in evaporator and total heat added to desorber bed during one complete cycle.

$$COP = \frac{Q_{EVP}}{Q_{1-2} + Q_{2-3}} \quad (19)$$

Following parameters are used for dynamic modelling.

In all the equations temperature T is in Kelvin, (K). The properties related to methanol are obtained by determining the best fit curve from the discrete values obtained, by using EES software, for methanol and activated carbon at various temperatures within the range 200 - 400 K [5]. Tab-2, gives thermo physical properties of heat transfer fluid used for simulation. Tab-3 shows operating parameters of the system.

**Table 2. Properties of water (Heat transfer fluid)**

Symbol	Parameter	Value	Unit
$\rho_w$	Density of water	1000	kg/m <sup>3</sup>
$\nu_w$	Kinematic viscosity of water	$0.3264 \times 10^6$	m <sup>2</sup> /sec
$c_{pw}$	Specific heat of water	4.203	kJ/kg°C
$\mu_w$	Dynamic viscosity of water	$0.3150 \times 10^3$	kg/m-sec
$k_w$	Thermal conductivity of water	0.6727	W/m-K

**Table 3. Operating parameters**

Symbol	Parameter	Value	Unit
$T_{hwi}$	Hot Water Inlet Temperature	90	°C
$T_C$	Condenser Temperature	35	°C
$T_E$	Evaporator Temperature	5	°C
$T_3$	Maximum Bed Temperature	80	°C
$\dot{m}_{hw}$	Mass Flow Rate of Hot Water	400	LPH
$\dot{m}_{cw}$	Mass Flow Rate of Cold Water	300	LPH

#### 4. Result and Discussion:

The results obtained from the mathematical model have been checked in the following ways:

- (i) The net desorbed mass during process 2 – 3 can be estimated as:  $\Delta x = \int_{T_2}^{T_3} \frac{dx}{dT} dT$ ; which is checked to be equal to  $(x_2 - x_3)$ , where  $x_2$  and  $x_3$  are estimated independently by eq. (6) for the given conditions of state points 2 and 3, respectively.
- (ii) Similarly, the net adsorbed mass during process 4 – 1 can be estimated as:  $\Delta x = \int_{T_4}^{T_1} \frac{dx}{dT} dT$ ; which is checked to be equal to  $(x_1 - x_4)$ , where  $x_1$  and  $x_4$  are estimated independently by eq. (6) for the given conditions of state points 1 and 4, respectively.
- (iii) Total heat added during the cycle is checked to be equal to the total heat rejected during the cycle. Thus  $(Q_{1-2} + Q_{2-3} + Q_{EVP})$  is checked to be equal to  $(Q_{3-4} + Q_{4-1} + Q_{COND})$ , where each of the heat transfer parameters have been estimated independently.

The simulated results in terms of heat and mass transfer rates, and total heat and mass transfers during each of the processes and also for the whole cycles are presented here. Results are also obtained for the time required to complete each of the processes and hence for completion of the cycle. Effects of initial bed temperature ( $T_1$ ) on different output parameters are also discussed.

Fig.3 shows the variation of bed temperature during the progress of the cycle for different initial bed temperatures ( $T_1$ ). The observations from this figure are as follows:

- The time period for completion of the cycle depends strongly on the initial temperature of the cycle and is varied from 20.41 h for  $T_1 = 30^\circ\text{C}$  -10.7 h for  $T_1 = 40^\circ\text{C}$ .
- The temperature at which desorption starts ( $T_2$ ) depends on the condenser pressure as well as on the mass ratio ( $x_1$ ) at the initial point (since  $x_2 = x_1$ ), which, in turn depends on the initial temperature ( $T_1$ ). Thus, the temperature for beginning of desorption ( $T_2$ ) changes with a change in  $T_1$ . It is observed the value of  $T_2$  varies from  $61.43^\circ\text{C}$  for  $T_1 = 30^\circ\text{C}$  and  $72.68^\circ\text{C}$  for  $T_1 = 40^\circ\text{C}$  (Fig. 3).
- During isosteric heating, initially the rate of heat addition is high and temperature of the bed increases at a faster rate, but as the bed temperature rises, the temperature difference between circulating hot water and the adsorber bed decreases, consequently the rate of heat transfer and the rate of change of temperature rise both decrease. The total time required for completion of the process 1-2 varies from 1.68 h (for  $T_1 = 30^\circ\text{C}$ ) - 2.37 h (for  $T_1 = 40^\circ\text{C}$ ).
- For the process 2-3, the heat transfer rate is very low due to the low temperature difference between circulating hot water and the adsorber bed and hence, the temperature rises very slowly. It is found that during this process, the increase of temperature of the bed is only between  $10^\circ\text{C}$ -  $19^\circ\text{C}$  but the duration of heating is between 4.23h and 8.53 h depending upon  $T_1$  of the cycle.
- It is observed that the slope of the temperature curve with time for process 1-2 is much steeper, compared to that for the process 2-3. This is attributed to the lower temperature difference between the hot water and the bed during the process 2-3 compared to that for process 1-2 and requirement of the heat of desorption during the process 2-3.
- The temperature at which adsorption starts ( $T_4$ ) depend on evaporator temperature and pressure and also on the maximum temperature of the bed ( $T_3$ ) and not on  $T_1$ . In Fig. 3, the value of  $T_4$  is  $46.56^\circ\text{C}$  for all three values of  $T_1$ .
- During cooling process 3-4, as the process progresses, the bed temperature decreases and hence the temperature difference between the bed and the cooling water also decreases. Therefore, heat transfer rate, and hence the rate of temperature drop, decrease with the progress of time during this process. However, duration of the process 3-4 is independent of  $T_1$  and is found to be around 1.8h for three values of  $T_1$ .



- During the process 4-1, the rate of heat transfer, and hence the rate of temperature drop decrease mainly due to (i) lower temperature difference between the bed and the cooling water, and (ii) heat released as ‘heat of adsorption’ is also to be removed along with sensible cooling of the bed. The isobaric cooling phase continues for a time period of 8.67h (for  $T_1 = 30^\circ\text{C}$ ) - 2.3h (for  $T_1 = 40^\circ\text{C}$ ).

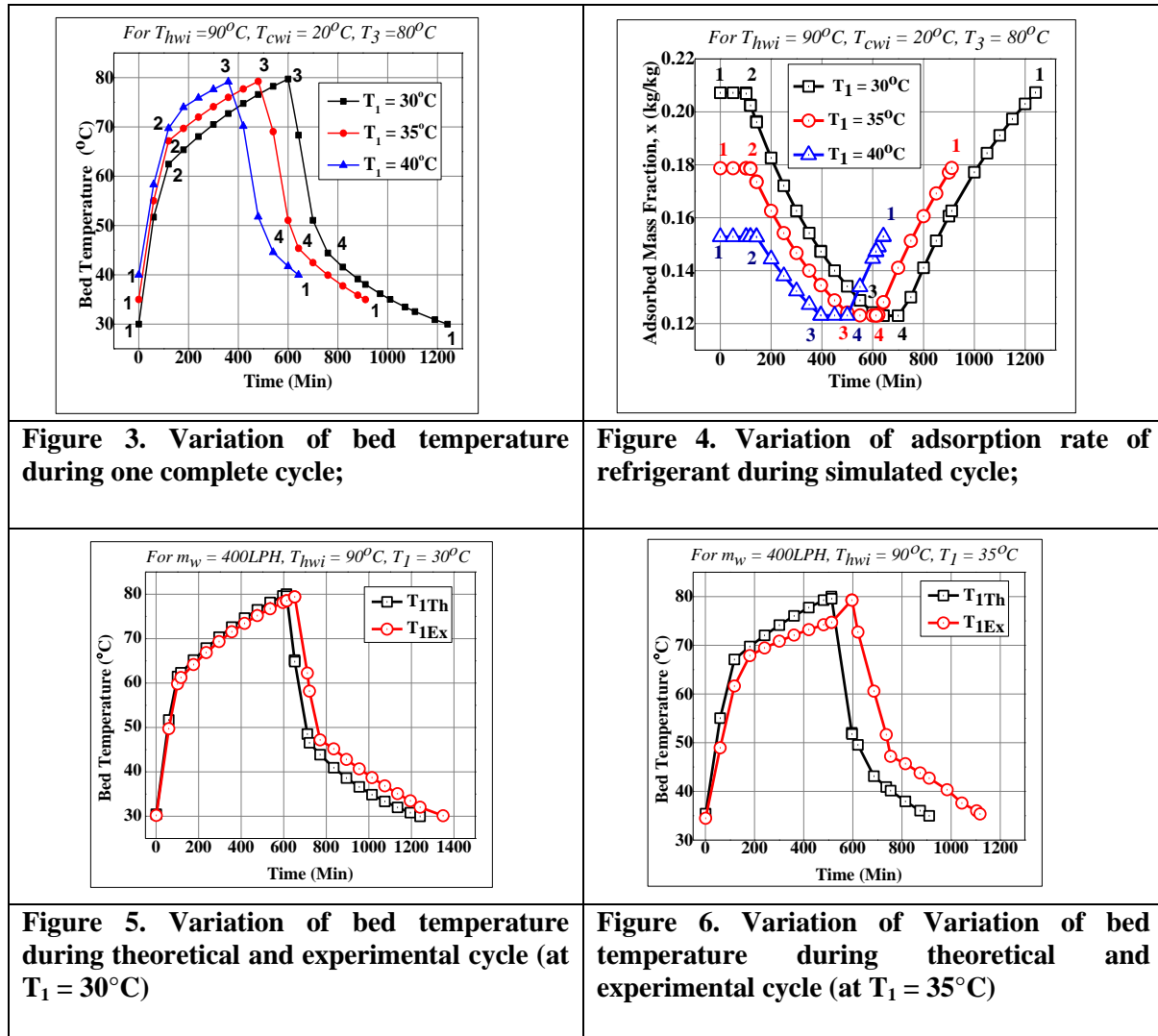
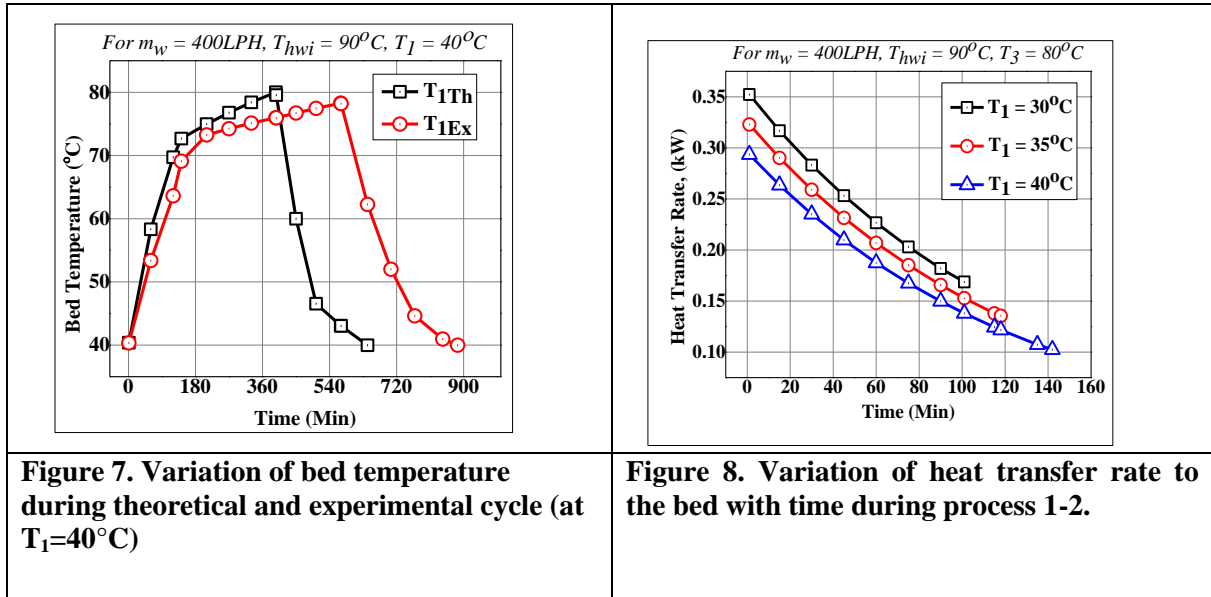


Fig. 4 shows the variation of the mass ratio of adsorbed mass as a function of time during the four processes of the cycle for three different initial bed temperatures ( $T_1$ ) of  $30^\circ\text{C}$ ,  $35^\circ\text{C}$  and  $40^\circ\text{C}$ . The observations from this figure are as follows:

- The adsorbed mass fraction of methanol ( $x_1$ ) at the beginning of the process is found to vary between 0.2072 kg/kg (for  $T_1 = 30^\circ\text{C}$ ) and 0.1528 kg/kg (for  $T_1 = 40^\circ\text{C}$ ). The minimum adsorbed mass fraction ( $x_3$ ) is independent of  $T_1$  and is found to be 0.1230 kg/kg at the end of desorption process.
- As the process, 2 – 3 progresses, rate of desorption tends to increase due to increase in bed temperature but it tends to decrease due to progressively lower value of adsorbed mass ( $x$ ) and also due to lower rate heat transfer. The net result of these effects, is found to decrease the rate of desorption very slowly (Fig. 4.).



**Figure 7. Variation of bed temperature during theoretical and experimental cycle (at  $T_1=40^\circ\text{C}$ )**

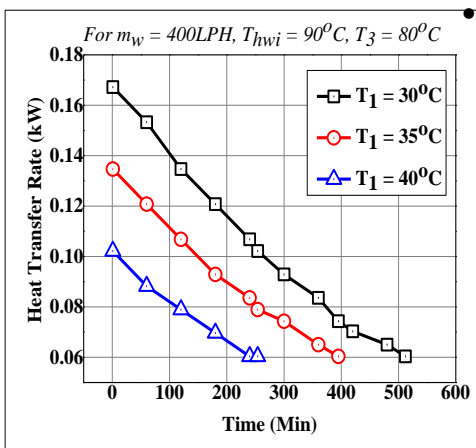
**Figure 8. Variation of heat transfer rate to the bed with time during process 1-2.**

- Similarly, as the process 4 – 1 progress, there is a decrease in bed temperature, an increase in the mass ratio of adsorbed refrigerant and decrease the rate of heat transfer. The net result of these effects is found to decrease the rate of adsorption, but very slowly.

Fig.5, 6 and 7 shows the influence of initial bed temperatures ( $T_1 = 30^\circ\text{C}, 35^\circ\text{C}, 40^\circ\text{C}$ ) on theoretical and practical cycle time. Due to more losses in experimental result, the cycle time is large compare to theoretical cycle time. For  $T_1 30^\circ\text{C}$ , the corresponding cycle time is 1349 min for the experimental cycle, which is large compare to others model. The time duration for the processes 1-3 (heating and desorption) and 3-1(cooling and adsorption) are 651 min and 698 min for  $T_1$  of  $30^\circ\text{C}$ . For  $T_1 40^\circ\text{C}$  minimum time duration of the cycle is observed. The time duration for the processes 1-3 (heating and desorption) and 3-1(cooling and adsorption) are 396 min and 246 min respectively. Here, it may be mentioned that the present model aims to predict the performance of an existing setup of adsorption refrigeration system and there is enough scope for improving performance and optimization of the system

Fig.8. represents the variation of the rate of heat transfer by hot water to the bed with time during process 1 – 2, for different values of  $T_1$ . As  $T_1$  increases, the following effects are observed:

- The corresponding value of  $T_2$  increases (Fig.3). The temperature change during process 1-2, ( $\Delta T = T_2 - T_1$ ) also increases. The heat addition to the bed during process 1-2 also increases (Fig. 9).
- The temperature difference between hot water and average bed temperature decrease, due to which the average rate of heat transfer decreases. The time required for bed temperature to reach to  $T_2$  increases(fig. 3.), due to increasing in temperature rise ( $\Delta T = T_2 - T_1$ ) and decrease in the average rate of heat transfer.



During the process 1-2, the average heat transfer rate with  $T_1 = 40^\circ\text{C}$ , is the minimum and it takes the maximum time to reach to temperature  $T_2$ .

During the process, 2 – 3, a variation of the rate of heat transfer to bed and bed temperature with time at different

values of  $T_1$  is shown in Fig. 9. With increase of value of  $T_1$ , the following effects are observed:

It is observed that for  $T_1=30^\circ\text{C}$ , the average heat transfer rate is higher due to lower average bed temperature and hence, higher average temperature difference.

- The temperature rise during the process ( $\Delta T = T_3 - T_2$ ) decreases since  $T_3$ , the maximum cycle temperature is kept fixed and  $T_2$  increases with increase in  $T_1$ . Consequently, the time required for completion of process 2-3 decreases due to lower temperature rise (Fig. 5.). For  $T_1 = 30^\circ\text{C}$ , time requires to reach  $T_3$  is the maximum (541mins).

**Figure 9. Variation of heat transfer rate to the bed with time during process 2 – 3**

Tab-4 compares theoretical and experimental heat transfer between different processes of adsorption cycle. It is observed that for process 1-2 and 2-3 experimental heat transfer is higher in comparison to theoretical heat transfer for increases of  $T_1$ . It is occurred due to heat loss to the surrounding from adsorber and hot water pipeline. It is observed that less amount of heat gain of cold water is occurred in experimental cycle compared to theoretical cycle. Variation of heat gain of cold water in experimental and theoretical cycle decrease with increases of  $T_1$ . Variation of heat lost in condenser between experimental and theoretical is varied between 7.5% and 14%. For  $T_1 = 30^\circ\text{C}$  refrigeration effect of the experimental cycle is reduced by 49% with compare to theoretical cycle. For  $T_1 = 40^\circ\text{C}$  this difference is very less because in higher value if  $T_1$  refrigeration effect also decreases. So in lower value, there is a less possibility of variation.

**Table 4. Results for the complete cycle ( $T_{\max} = 80^\circ\text{C}$ ,  $T = 35^\circ\text{C}$  and  $T_E = 5^\circ\text{C}$ )**

Parameters	For $T_1 = 30^\circ\text{C}$		For $T_1 = 35^\circ\text{C}$		For $T_1 = 40^\circ\text{C}$	
	Pred.	Expt	Pred.	Expt	Pred.	Expt
Total heat transfer during process 1 – 2 (kJ)	1500.12	2262.63	1518.19	2276.43	1536.81	2968.64
Total heat transfer during process 2 – 3 (kJ)	3273.85	4725.07	2208.89	3945.92	1207.27	2144.90
Total heat transfer during process 3 – 4 (kJ)	1563.51	1443.37	1563.51	1473.24	1563.51	1483.9
Total heat transfer during process 4 – 1 (kJ)	3069.08	2306.94	2064.94	2008.44	1129.52	709.56
Total time for the cycle (mins)	1241	1349	911	1176	642	884
Maximum adsorbed mass, $x_1$ (kg/kg)	0.21	0.20	0.18	0.17	0.15	0.14
Minimum adsorbed mass, $x_3$ (kg/kg)	0.12	0.12	0.12	0.12	0.12	0.12
Heat transfer in condenser (kJ)	2234.04	1922.59	1482.62	1127.07	795.63	735.89
Heat transfer in evaporator (kJ)	2081.95	1394.27	1376.53	1200.69	736.00	704.39
COP	0.44	0.21	0.37	0.19	0.27	0.16
SCC (kJ/kg)	94.63	63.38	62.57	54.58	33.45	32.02

## 5. Conclusion:

The present study has demonstrated the influence of inlet bed temperature ( $T_1 = 30, 35, 40^\circ\text{C}$ ) on heat and mass transfer performances of an adsorption refrigeration system. This study gives a clear understanding of the dynamic adsorber behavior, heat addition, and rejection during different

processes. The estimated highest specific cooling capacity and COP of the system are found to be 94.63 kJ/kg of adsorbent and 0.44 respectively for 30°C of  $T_1$ . But the corresponding cycle time is 1241 min (1349 min experimental cycle), which is large compare to others model. The time duration for the processes 2-3 (desorption) and 4-1(adsorption) are 512min and 520 min for  $T_1$  of 30°C. Here, it may be mentioned that the present model aims to predict the performance of an existing setup of adsorption refrigeration system and there is enough scope for improving performance and optimization of the system. The time duration can be reduced by augmenting heat transfer rates between adsorber bed, heat-exchanger fluid (water) and refrigerant. On the other hand, heat transfer rate can be increased by increasing equivalent thermal conductivity and heat transfer surface area of the bed, the thermal conductivity of heat exchanger fluid and refrigerant. In the existing model, fins can be used or some metallic powder can be mixed with an adsorbent bed to increase heat transfer rate. In future, the focus will be on more specific design to enhance heat and mass transfer rate inside the adsorber bed.

### Nomenclature:

$A_o$	-Outer surface area of copper tube, [m <sup>2</sup> ]
$C$	-Constant of Clausius –Clapeyron equation
$c_{p,liq}$	-Specific heat of liquid refrigerant at a constant pressure, [kJ/kg – K]
$c_{v,ref}$	-Specific heat of gas refrigerant at a constant volume, [kJ/kg- K]
$c_{p,ref}$	.Specific heat of gas refrigerant at a constant pressure, [kJ/kg- K]
$c_{st}$	-Specific heat of steel,[kJ/kg- K]
$c_{cu}$	-Specific heat of copper,[J/kg- K]
$c_{ac}(T)$	-Specific heat (function of temperature) of activated carbon, [kJ/kg- K]
$c_{pw}$	-Specific heat of hot water, [kJ/kg- K]
$k, n$	-Adsorptive parameters of adsorbent- adsorbate pair
$\Delta h_{id}$	-Heat of desorption, [kJ/kg]
$\Delta h_{ia}$	-Heat of adsorption, [kJ/kg]
$L_{ref}$	-Latent heat of refrigerant, [kJ/kg]
$h_{ref}$	-Enthalpy of refrigerant, [kJ/kg]
$m_{ac}$	-Mass of adsorbent, [kg]
$m_{cu}$	-Mass of copper, [kg]
$\dot{m}_{cw}$	-Mass flow rate of cold water, [kg/s]
$\dot{m}_{hw}$	-Mass flow rate of hot water, [kg/s]
$m_{st}$	-Mass of stainless steel, [kg]
$P_C$	-Pressure of adsorbate at condenser, [Pa]
$P_E$	-Pressure of adsorbate at evaporator, [Pa]
$\dot{Q}_{ad}$	-Rate of sensible heat of adsorbent, [kJ/s]
$\dot{Q}_{ads}$	-Rate of adsorption heat of refrigerant,[kJ/s]
$\dot{Q}_{bed}$	-Rate of sensible heat of adsorber bed, [kJ/s]
$\dot{Q}_{COND}$	-Rate of heat rejection at condenser, [kJ/s]
$\dot{Q}_{des}$	-Rate of desorption heat of refrigerant, [kJ/s]
$Q_{EVP}$	-Heat exchange in evaporator, [kJ]
$\dot{Q}_h$	-Heat transfer rate between hot water and desorber bed, [kJ/s]
$\dot{Q}_{ref}$	-Rate of sensible heat of refrigerant, [kJ/s]
$R$	-Gas constant for refrigerant, [kJ/kg-K]
$T$	-Average temperature of the adsorber bed, [K]
$T_1$	-Temperature at the end of adsorption, [K]

$T_2$	-Temperature at the beginning of desorption, [K]
$T_3$	-Temperature at the end of desorption, [K]
$T_4$	-Temperature at the beginning of adsorption, [K]
$T_5$	-Temperature of refrigerant leaving the condenser, [K]
$T_6$	-Temperature of refrigerant leaving the evaporator, [K]
$T_C$	-Saturation temperature of the condenser, [K]
$T_E$	-Saturation temperature of the evaporator, [K]
$T_{cwi}$	-Inlet temperature of cold water, [K]
$T_{hwi}$	-Inlet temperature of hot water, [K]
$T_{hwo}$	-Outlet temperature of hot water, [K]
$T_{Sat}$	- Saturation temperature of the adsorbate corresponding to the bed pressure
$x$	-Mass ratio of adsorbed mass to that of the adsorbent, [kg/kg]
$x_o(T_s)$	-Limiting mass ratio at saturation temperature, [kg/kg]
$U_o$	-The overall heat transfer coefficient, [kW/m <sup>2</sup> -K]

### References:

- [1]Habib, K., et al. Study of various adsorbente–refrigerant pairs for the application of solar driven adsorption cooling in tropical climates,*Applied Thermal Eng*, 72(2014), pp. 266–74.
- [2]Wang, L.W., et al. The performance of two adsorption ice making test units using activated carbon and a carbon composite as adsorbents,*Carbon 44* (2006), pp. 2671–80.
- [3]Naef, A.A.,al. Thermal analysis and modeling study of an activated carbon solar adsorption ice maker, *Energy Conversion and Management*,100 (2001), pp. 310–323.
- [4] Hassan, H.Z, Mohamad, A.A., Thermo dynamic analysis and theoretical study of a continuous operation solar-powered adsorption refrigeration system, *Energy 61* (2013),pp.167-178.
- [5]Sur, A, Randip, K.D., Numerical Modeling and Thermal Analysis of an Adsorption Refrigeration System, *International Journal of Air-Conditioning and Refrigeration 23* (2015), 4, pp.15500331-11.
- [6]Chekirou, W., et.al. Dynamic modelling and simulation of the tubular adsorber of a solid adsorption machine powered by solar energy,*Int J Refrig.*39 (2014), pp.137–51.
- [7] Gaglino A, Patania F, Nocera F, Galesi A, performance assesment of a solar assisted desiccant cooling system, *Thermal Science 18* (2014), 2, pp. 563-576.
- [8] Jani D B, Mishra.M, Sahoo P K, Solid desiccant air conditionig – A state of the art review, *Renewable and sustainable energy 60* (2016), pp. 1451-1469